Analyst

PAPER

Cite this: *Analyst*, 2016, **141**, 5127

Rapid, accurate, and comparative differentiation of clinically and industrially relevant microorganisms *via* multiple vibrational spectroscopic fingerprinting†

Howbeer Muhamadali,[a] Abdu Subaihi,[a] Mahsa Mohammadtaheri,[b] Yun Xu,[a] David I. Ellis,[a] Rajesh Ramanathan,[b] Vipul Bansal[b] and Royston Goodacre*[a]

Despite the fact that various microorganisms (*e.g.*, bacteria, fungi, viruses, *etc.*) have been linked with infectious diseases, their crucial role towards sustaining life on Earth is undeniable. The huge biodiversity, combined with the wide range of biochemical capabilities of these organisms, have always been the driving force behind their large number of current, and, as of yet, undiscovered future applications. The presence of such diversity could be said to expedite the need for the development of rapid, accurate and sensitive techniques which allow for the detection, differentiation, identification and classification of such organisms. In this study, we employed Fourier transform infrared (FT-IR), Raman, and surface enhanced Raman scattering (SERS) spectroscopies, as molecular whole-organism fingerprinting techniques, combined with multivariate statistical analysis approaches for the classification of a range of industrial, environmental or clinically relevant bacteria (*P. aeruginosa*, *P. putida*, *E. coli*, *E. faecium*, *S. lividans*, *B. subtilis*, *B. cereus*) and yeast (*S. cerevisiae*). Principal components-discriminant function analysis (PC-DFA) scores plots of the spectral data collected from all three techniques allowed for the clear differentiation of all the samples down to sub-species level. The partial least squares-discriminant analysis (PLS-DA) models generated using the SERS spectral data displayed lower accuracy (74.9%) when compared to those obtained from conventional Raman (97.8%) and FT-IR (96.2%) analyses. In addition, whilst background fluorescence was detected in Raman spectra for *S. cerevisiae*, this fluorescence was quenched when applying SERS to the same species, and conversely SERS appeared to introduce strong fluorescence when analysing *P. putida*. It is also worth noting that FT-IR analysis provided spectral data of high quality and reproducibility for the whole sample set, suggesting its applicability to a wider range of samples, and perhaps the most suitable for the analysis of mixed cultures in future studies. Furthermore, our results suggest that while each of these spectroscopic approaches may favour different organisms (sample types), when combined, they would provide complementary and more in-depth knowledge (structural and/or metabolic state) of biological systems. To the best of our knowledge, this is the first time that such a comparative and combined spectroscopic study (using FT-IR, Raman and SERS) has been carried out on microbial samples.

Received 15th April 2016,
Accepted 7th July 2016

DOI: 10.1039/c6an00883f

www.rsc.org/analyst

Introduction

The huge biodiversity, combined with the wide range of biochemical capabilities of micro-organisms, have always been the driving force behind their large number of applications in various fields of science, technology, and industry, including: agriculture,[1] food production and processing,[2,3] biotechnology,[4,5] bioremediation,[6,7] and more recently, synthetic biology.[8,9] The presence of such microbial diversity, which results in clear chemical differences between different bacterial genera and species requires the development of rapid, accurate and sensitive physicochemical techniques allowing for the detection, identification and classification of such highly beneficial organisms, which are potentially of huge importance for food safety,[10,11] clinical medicine, the environment,[12,13] as well as the production of a whole range of compounds within the setting of synthetic biology.

Although traditional techniques such as phenotypic and serological tests are still used in clinical settings for bacterial

[a]*School of Chemistry, Manchester Institute of Biotechnology, University of Manchester, Manchester, UK. E-mail: roy.goodacre@manchester.ac.uk; Tel: +44(0) 161 306-4480*

[b]*Ian Potter NanoBioSensing Facility, NanoBiotechnology Research Laboratory, School of Science, RMIT University, Melbourne, Australia*

†Electronic supplementary information (ESI) available. See DOI: 10.1039/c6an00883f

identification, these approaches are considered time-consuming (generally between 24–72 h), laborious and often provide limited accuracy.[14] In addition to these approaches, molecular biology approaches such as 16S or 18S ribosomal DNA or RNA[15,16] amplification combined with sequencing assays, and analytical techniques, most notably matrix-assisted laser desorption ionisation time-of-flight mass spectrometry (MALDI-TOF-MS)[17,18] are also considered as viable options for this task. However, in order to achieve identification at subspecies level using 16S or 18S rRNA sequencing techniques, full genome sequence of the organisms are required, and perhaps importantly, these techniques are not ideally suited for field applications.[19,20]

During the past few decades the application of spectroscopy-based techniques, such as molecular fingerprinting approaches, for microbial identification and classification has attracted a lot of attention.[16,18–20] Fourier transform infrared (FT-IR) spectroscopy, a vibrational spectroscopic technique based on the interaction of IR light with the molecular bonds in a sample,[21] is a low cost, rapid (<1 min per sample) and high-throughput fingerprinting technique with demonstrated utility in various applications including those within, but not exclusive to, the food safety,[22,23] clinical,[18] biotechnology[24–26] and environmental[27,28] arenas. However, one of the limitations of FT-IR for investigation of biological systems is the strong absorbance of water in such samples, which is overcome in some cases by subtraction of the water signal, drying the sample or using alternative IR-based techniques such as the less sensitive near-IR (NIR), or attenuated total reflectance (ATR) sampling accessories or probes.[29]

As a complementary technique to FT-IR, Raman spectroscopy is considered an ideal method for the analysis of aqueous samples as water is a weak Raman scatterer, and the resultant Raman spectra tend to be more information rich in terms of the spectra having sharper peaks than FT-IR spectra.[30] However, one of the known limitations of this vibrational technique is that the Raman scattering is inherently weak. Over the past few decades this has been to a degree overcome by the development of new signal enhancement methods (*e.g.* surface enhanced Raman scattering (SERS) and resonance Raman techniques), as well as significant advancements in instrumentation (*e.g.*, charged-coupled devices and laser technology), and computation. These improvements have contributed towards the various applications of Raman spectroscopy in many different areas of microbiology, including: food safety,[31–34] medical,[35,36] cell sorting (Raman tweezers),[37] as well as classification of fixed and live bacteria at colony,[38,39] spore,[40] and single cell levels.[41–44] Alternatively, SERS, as a Raman enhancement technique (with a typical enhancement factor of 10^4–10^6; ref. 45), has also become an increasingly attractive approach as it allows for the rapid, sensitive, selective and label-free detection of various biomolecules. Such advantages have contributed towards its popularity and broad range of applications such as the detection of biomarkers for various diseases,[46,47] DNA detection,[48–50] monitoring enzyme activity,[51,52] and in particular for detection,[53] quantification,[54] and classification of microbial cells.[55–57] For an overview on fundamental aspects and applications of SERS, the reader is directed to the following general reviews with excellent coverage of the area.[19,58–60]

In this study, we employed FT-IR and conventional Raman spectroscopies, and surface enhanced Raman scattering, as physicochemical fingerprinting techniques, combining these with multivariate statistical analysis approaches for the rapid and accurate classification of a range of bacterial (*P. aeruginosa*, *P. putida*, *E. coli*, *E. faecium*, *S. lividans*, *B. subtilis*, *B. cereus*) and yeast (*S. cerevisiae*) cells. To the best of our knowledge, this is the first time that such a combined and comparative study (using FT-IR, Raman and SERS) has been carried out on microbial samples.

Materials and methods

Bacteria and yeast growth conditions

All chemicals and reagents were purchased from Sigma-Aldrich (Sigma Aldrich, UK) unless otherwise stated. A list of all the microorganisms used in this study, along with their characteristics, is provided in Table 1. All microorganisms used in this study were sub-cultured three times on the relevant agar medium, to ensure purity and phenotypic stability, before being used for inoculum preparation. Five biological replicates of all microbes were cultured.

Escherichia coli, *Bacillus subtilis*, *B. cereus* and *Enterococcus faecium* were inoculated into 50 mL of nutrient broth, to a final $OD_{600\ nm}$ of 0.1, and incubated at 37 °C with 200 rpm shaking using a Multitron standard shaker incubator (INFORS-HT Bottmingen Switzerland). *Pseudomonas putida*

Table 1 Microorganisms and their specific growth conditions used in this study

Genus and species	Organism	Gram stain	Incubation temperature (°C)	Growth media
Escherichia coli	Bacterium	−	37	Nutrient broth
Pseudomonas putida	Bacterium	−	30	Nutrient broth
Pseudomonas aeruginosa	Bacterium	−	30	Nutrient broth
Saccharomyces cerevisiae	Yeast	n/a	30	YPD
Streptomyces lividans	Bacterium	+	30	Phage
Bacillus subtilis	Bacterium	+	37	Nutrient broth
Bacillus cereus	Bacterium	+	37	Nutrient broth
Enterococcus faecium	Bacterium	+	37	Nutrient broth

This journal is © The Royal Society of Chemistry 2016

and *Pseudomonas aeruginosa* were grown under identical conditions except that the incubator was set to 30 °C. *Saccharomyces cerevisiae* was inoculated into 50 mL of yeast extract-peptone-dextrose (YPD) medium followed by incubation at 30 °C with 200 rpm shaking. Precultures of *Streptomyces lividans* TK24 were prepared by inoculating 50 mL of phage medium with a dense spore stock (10^8 spores per mL) followed by incubation at 30 °C with 280 rpm shaking for 24 h.[25] The resultant vegetative mycelial cells were harvested by centrifugation (4000*g* at 4 °C for 10 min), washed using sterile normal saline solution, and inoculated into 50 mL of phage medium in 250 mL baffled flasks and incubated at 30 °C with 280 rpm shaking, to achieve homogeneous growth and avoid any clump formation.

Sample preparation

Biomass from all the samples was harvested at late exponential phase by centrifugation at 4000*g* for 10 min at 4 °C using a MicroCL 17R microcentrifuge (Thermo Fisher Scientific Inc., UK). The supernatant was discarded and the biomass washed twice using sterile physiological saline solution (0.9% NaCl) to remove any residual compounds from the medium, as previously reported.[24,41] All washed samples were resuspended in saline solution and normalised according to their $OD_{600\ nm}$ (~15).

FT-IR analysis

Samples were spotted as 20 μL aliquots onto a FT-IR silicon 96 well plate and heated to dryness at 55 °C for ~30 min. FT-IR spectral data were collected in absorbance mode in the Mid-IR range (4000–600 cm^{-1}) on a Bruker Equinox 55 infrared spectrometer (Bruker Optics Ltd, Coventry, UK), as 64 co-adds with 4 cm^{-1} resolution, in triplicate (analytical replicates) from separate regions of each of the sample spots.[61] FT-IR spectral data were normalised using standard normal variate (SNV) transformation,[62] followed by replacement of the CO_2 peaks with a trend (2400–2275 cm^{-1}).

Raman analysis

Samples were spotted onto prewashed calcium fluoride (CaF_2) discs in 5 μL aliquots and dried in a desiccator at room temperature. Raman analysis was carried out on a Renishaw inVia Raman microscope (Renishaw Plc., Gloucestershire, UK) equipped with a 785 nm laser. The instrument was calibrated with a silicon wafer focused under a ×50 objective, where a static spectrum centered at 520 cm^{-1} for 1 s at 10% power was collected. Spectral data were collected using the GRAMS WiRE 3.4 software (Galactic Industries Corp. Salem, NH). All spectra were acquired using 20 s exposure time, three accumulations and 600 l mm^{-1} grating, in the 2233–489 cm^{-1} spectral range, and the laser power was adjusted on the sample to ~30 mW.[41] All collected Raman spectral data were baseline corrected and normalised using SNV transformation.[62]

Synthesis of Ag nanoparticles (AgNPs)

For SERS, AgNPs were synthesised using amino acid tyrosine as a reducing and capping agent, as shown in previous studies.[63,64] Briefly, 100 mL aqueous solution comprising of 0.1 mM tyrosine and 0.1 mM KOH were heated to boiling point. Under alkaline boiling conditions, 0.1 mM equivalent of Ag^+ ions ($AgNO_3$) were added to the above solution with subsequent boiling for a further 5 min. This resulted in a yellow coloured solution consisting of tyrosine capped AgNPs. Rotary vacuum evaporation was used to concentrate AgNPs solution 10 times. These NPs solutions were found to be highly stable even after the evaporation process, signifying the strong tyrosine capping. The concentrated solution of AgNPs was dialysed overnight against deionised MilliQ water using 12 kDa molecular weight cut-off cellulose dialysis membranes, followed by exchange of water twice, in order to remove the excess amounts of KOH, potentially unreduced Ag^+ ions and unbound tyrosine. The concentration of silver in AgNPs was determined using Atomic Absorption Spectroscopy (AAS) (Varian, Inc. Middelburg, Netherlands).

Nanoparticle characterisation

The homogeneous colloidal solution obtained after removal of unbound amino acids and ions was characterized by UV–visible absorbance spectroscopy using an Envision multi-label plate reader (PerkinElmer) (Fig. 1A). Samples for transmission electron microscopy (TEM) were prepared by drop-coating the solutions on to carbon-coated copper grids, followed by TEM measurements using a JEOL 1010 TEM instrument operated at an accelerating voltage of 100 kV. Dynamic light scattering (DLS) (Fig. S1†) and zeta potential measurements of AgNPs solution were carried out using a Malvern Nano-Zs/Zen3600 Zetasizer instrument. TEM image (Fig. 1B) of the AgNPs displayed acceptable size distribution and average particle size of 50 nm (±5 nm). Using AAS the final concentration of Ag in the prepared AgNPs solution was measured to be ~537 μM, while the zeta-potential, a measure of charge stability and particle interaction,[65] was −28.5 mV, suggesting moderate stability of the prepared nanoparticles.

SERS analysis

SERS analysis was carried out using a 785 nm laser on a Renishaw inVia Raman microscope (Renishaw Plc., Gloucestershire, UK). Instrument calibration procedure was undertaken

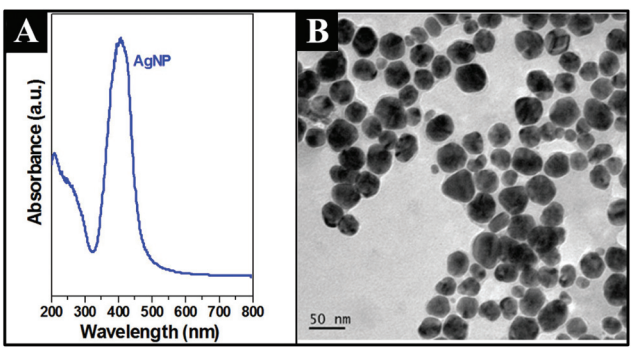

Fig. 1 UV-Vis absorption spectra (A), and TEM image (B) of the tyrosine capped AgNP solution, showing acceptable homogeneity and size distribution.

as detailed above. An equal volume (10 μL) of sample and AgNP solution were mixed in a sterile microcentrifuge tube, and from this mixture a 5 μL aliquot was spotted onto pre-washed CaF_2 discs and dried at room temperature in a desiccator. SERS spectral data were collected using a ×50 objective lens, 10 s exposure time and the motorized xy stage programmed to scan 56 spectra in a 8 × 7 grid with a step size of ~1 μm. Due to the randomly fluctuating nature of the SERS signal, as a result of either no SERS (Raman only from areas void of nanoparticles) or hot spots,[55,66] the collected spectral data required a pre-processing step prior to being used for construction of the classification models. Therefore, a strategy was employed by which the spectral data with saturated signal were excluded, a similar process has been adopted before for SERS of bacteria.[55] The remaining data were then normalised using SNV transformation, and subsequently subjected to robust-PCA[67] to identify the outliers which were also excluded. A schematic overview of these procedures is provided in Fig. 2.

Data analysis

MATLAB version 2013a (The Mathworks Inc., Natwick, USA) was used to carry out all the statistical analysis in this study. All preprocessed spectral data were subjected to principal component-discriminant function analysis (PC-DFA), using the first 20 PCs,[68] a supervised discriminatory statistical method that uses *a priori* knowledge (species information) to minimise within class variance, while maximising between class variance. Hierarchical cluster analysis (HCA) was then applied to the average of the PC-DFA scores (the first three scores retained) of the analytical replicates of each class (different species), to facilitate the visualisation of the distance between each of the clusters. In order to assess the unbiased capability of the models generated for discrimination of the spectral data, partial least squares-discriminant analysis (PLS-DA)[69] with bootstrapping (1000 iterations) validation was applied.[70] In each iteration, *n* (*n* is the total number of samples) samples were randomly selected *with replacement* (*i.e.* one sample can be selected multiple times) from the spectral data set and used as the training set, while the samples that had not been selected (due to the fact that a sample can be selected multiple times) were used as the test set.[69] The PLS-DA model was built on the training set and applied to the test set. The accuracy of the predictions on only the test set was then recorded. This process had been repeated 1000 times for each spectral data set and the prediction accuracies of the 1000 randomly generated test sets were then averaged and reported.[71]

Results

The average of all spectra collected using three spectroscopic techniques employed in this study are presented in Fig. 3. Due to the multivariate nature of the collected spectral data, simple visible discrimination of the spectra could not be achieved, thus several chemometrics approaches were employed to generate (with suitable validation) reliable classification models for each of the datasets. The results of each of the vibrational spectroscopies will be discussed in turn.

FT-IR fingerprints

PC-DFA scores plot of the FT-IR spectral data (Fig. 4A and B) demonstrated clear separation of *S. cerevisiae* from all other samples based on DF1. This is of course as expected as *S. cerevisiae* are eukaryotic yeast cells while all other samples are prokaryotic bacterial cells. In addition, the two *Bacillus* species clustered away from all other bacterial samples, on the positive side of DF2, while *E. coli*, *P. putida*, *P. aeruginosa* and *S. lividans* clustered closely on the negative side (Fig. 4B). These findings are also evident from the HCA dendogram constructed from the PC-DFA scores (Fig. 5A). However, it is worth noting that according to DF3 on the 3D PC-DFA scores plot (Fig. 4A), *S. lividans* is clearly separated from *E. coli* and both *Pseudomonas* species (all three are Gram-negative bacteria), while *B. subtilis* can also be distinguished from *B. cereus* using DF3.

According to the DF1 and DF2 loadings plots (Fig. S2A†) the most significant peaks contributing to such clustering patterns include: fatty acid vibrations at 2924 and 2853 cm^{-1} (CH_2, asymmetric and symmetric stretching respectively), esters at 1740 cm^{-1} (C═O, stretching), amide I at 1665 (C═O, stretching) and amide II at 1540 cm^{-1} (combination of C–N stretching and N–H bending), and other vibrational bands in the so called fingerprint region (1500–500 cm^{-1}).[41,72]

Next PLS-DA was used to try to classify the different microorganisms. In this approach we used binary encoding in the PLS2 analyses and as there were eight microbes to be identified a vector of '0's was used where '1' was employed for the correct identity; that is to say, for the identification of the 3rd microorganism (*E. coli* in this case; Table S1†) the encoding would be

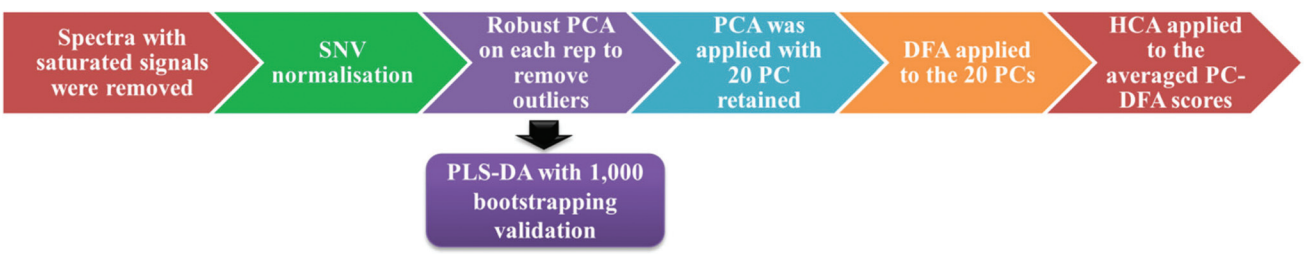

Fig. 2 Schematic overview of the procedures applied for the analysis of SERS spectral data.

This journal is © The Royal Society of Chemistry 2016

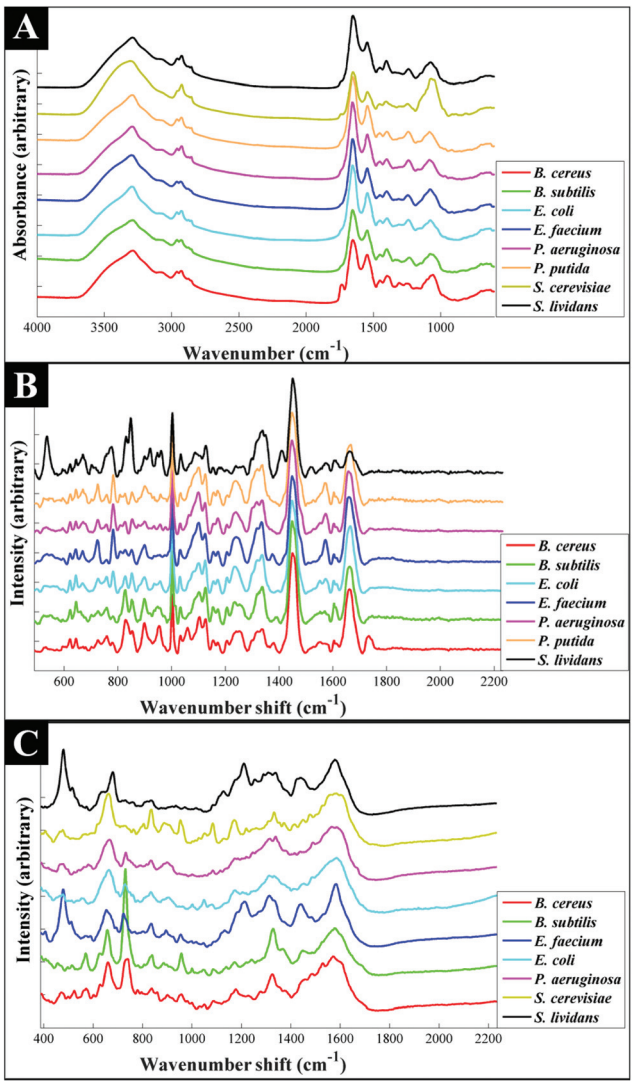

Fig. 3 Typical FT-IR (A), Raman (B) and SERS (C) spectra of the samples investigated in this study. All spectra were normalized using SNV transformation. Each spectrum represent the average of all biological (n = 5) and analytical replicates of that class (species).

"0, 0, 1, 0, 0, 0, 0, 0". The accuracy of predictions was assessed using bootstrapping (n = 1000) and the resultant confusion matrix (Fig. 6A) generated from PLS-DA confirmed the high accuracy of the generated models with prediction accuracies between 92.6–99.9%, and an overall average of 96.19% (Table S1†).

Raman fingerprints

Despite multiple attempts of optimisation using the 785 nm laser (*e.g.*, using various biomass concentrations, laser power and acquisition time), *S. cerevisiae* spectra contained high background fluorescence and unclear spectral features. Fluorescence is known to be a problem with yeast[73] and potentially can be overcome using the anti-Stokes scattering (although this is considerably weak), or better still, to employ SERS (*vide infra*). Thus, Raman spectral data of *S. cerevisiae* were excluded from further analysis. PC-DFA scores plot (Fig. 4C and D) of the remaining Raman spectral data displayed clear separation of all the species. *S. lividans* clustered away from all other samples, according to DF1 (Fig. 4D), while DF2 separated *E. coli*, *E. faecium* and *Pseudomonas* spp., from *S. lividans* and *Bacillus* spp.

Once again the 3D PC-DFA scores plot (Fig. 4C), separated the samples down to subspecies level, by which *B. subtilis*, *B. cereus*, *P. putida* and *P. aeruginosa* were further separated into distinct clusters. Using the DF1 and DF2 loadings plot (Fig. S2B†), the significant Raman vibrational bands were identified as: esters at 1731 cm^{-1} (C═O, stretching), amide I at 1651 cm^{-1} (C═O, stretching), lipids and nucleic acids at 1484 cm^{-1} (C–H, deformation), proteins at 1375 cm^{-1}, tyrosine (ring breathing) and/or nucleic acids (O–P–O, stretching) at 826 cm^{-1}, and a combination cytosine and uracil at 782 cm^{-1} (C═O, C–N and ring deformations).[41,72]

The HCA dendogram (Fig. 5B) of the Raman PC-DFA scores also exhibited this clear separation. Validation of the PLS-DA classification models (Fig. 6B), generated using Raman spectral data confirmed the accuracy and validity of the model (between 95.3–99.9%) with an average prediction accuracy of 97.8% (Table S2†).

SERS fingerprints

Unlike Raman, SERS spectra of *S. cerevisiae* provided detailed features (Fig. 3C) showing that the nanoparticles had caused an enhancement and had quenched fluorescence.[74] By contrast, SERS spectra obtained from *P. putida* samples contained high background fluorescence, possibly due to interaction of an exopolysaccharide capsule surrounding the cell with the surface-bound tyrosine specifically,[75] as such effect was not observed when using hydroxylamine-reduced Ag NPs (Fig. S3†). Therefore these spectral data were excluded from further analysis.

PC-DFA scores plot of the SERS spectral data displayed clear separation of all samples (Fig. 4E and F), the two *Bacillus* spp. were separated from all other samples based on DF1. Although *S. cerevisiae* are yeast cells with different biochemical composition compared to that of bacterial cells, and despite any prior assumptions, these samples clustered closely with *S. lividans*. It was clear that in comparison to FT-IR and Raman data (Fig. 4) that the clustering of the biological replicates was not so tight and this suggests that these data have higher variability. On further inspection, the 3D PC-DFA scores plot of the SERS spectral data (Fig. 4E), revealed that the Gram-positive bacteria (*E. faecium*, *S. lividans*, *B. subtilis*, and *B. cereus*) are generally clustered on the positive side of DF2, while the Gram-negative bacteria (*E. coli*, and *P. aeruginosa*) are on the negative side of DF2. According to the DF2 loadings plot (Fig. S2C†), the main vibrational bands contributing to this separation that have been observed in SERS of microorganisms include: carbohydrates at 486 cm^{-1},[76] proteins at 681 cm^{-1} (C–S stretching and C–C twisting),[77] polysaccharides at 730 cm^{-1} (*N*-acetyl-D-glucosamine and *N*-acetylmuramic acid),[55,78] tyrosine at 831 cm^{-1},[76,78] and lipids at 1447 cm^{-1} (CH_2 deformation).[78]

The HCA dendogram of the SERS PC-DFA scores (Fig. 5C), demonstrates a clearer image of this clustering pattern, whilst

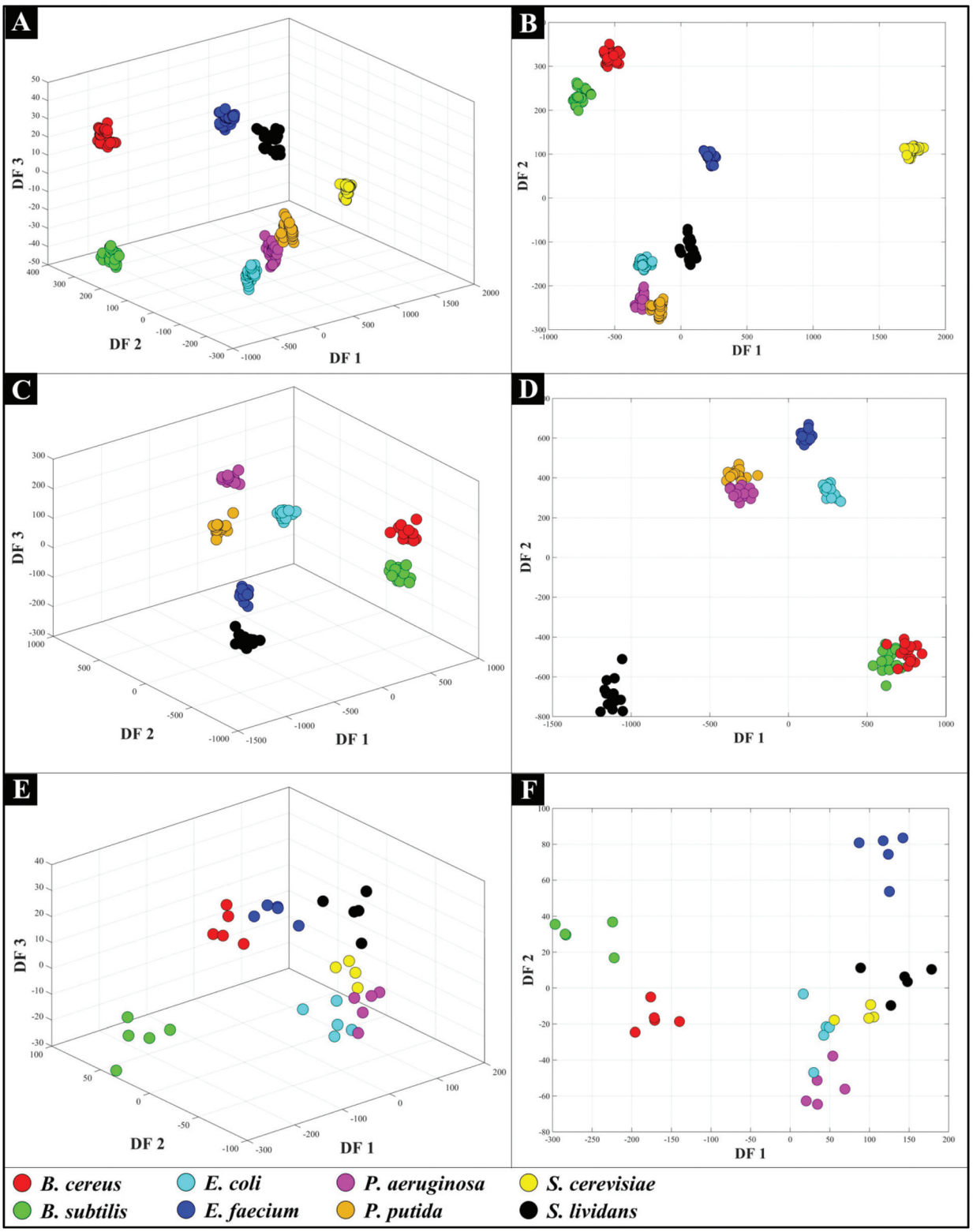

Fig. 4 PC-DFA scores plots of spectral data generated *via* FT-IR (A, B), Raman (C, D), and SERS (E, F) spectroscopic analysis of the different microbial samples. Different coloured symbols represent the different species, and the coding for this is provided in the figure.

it is evident that the two Gram-negative species *E. coli* and *P. aeruginosa* can not be differentiated, presumably due to the similarity in the cell wall of these two *Enterobacteriaceae*, where it is known that the majority of the SERS signal arises from.[19,55] Finally the PLS-DA classification model generated using SERS spectra provided lower accuracy (67.4–85.7%) com-

 This journal is © The Royal Society of Chemistry 2016

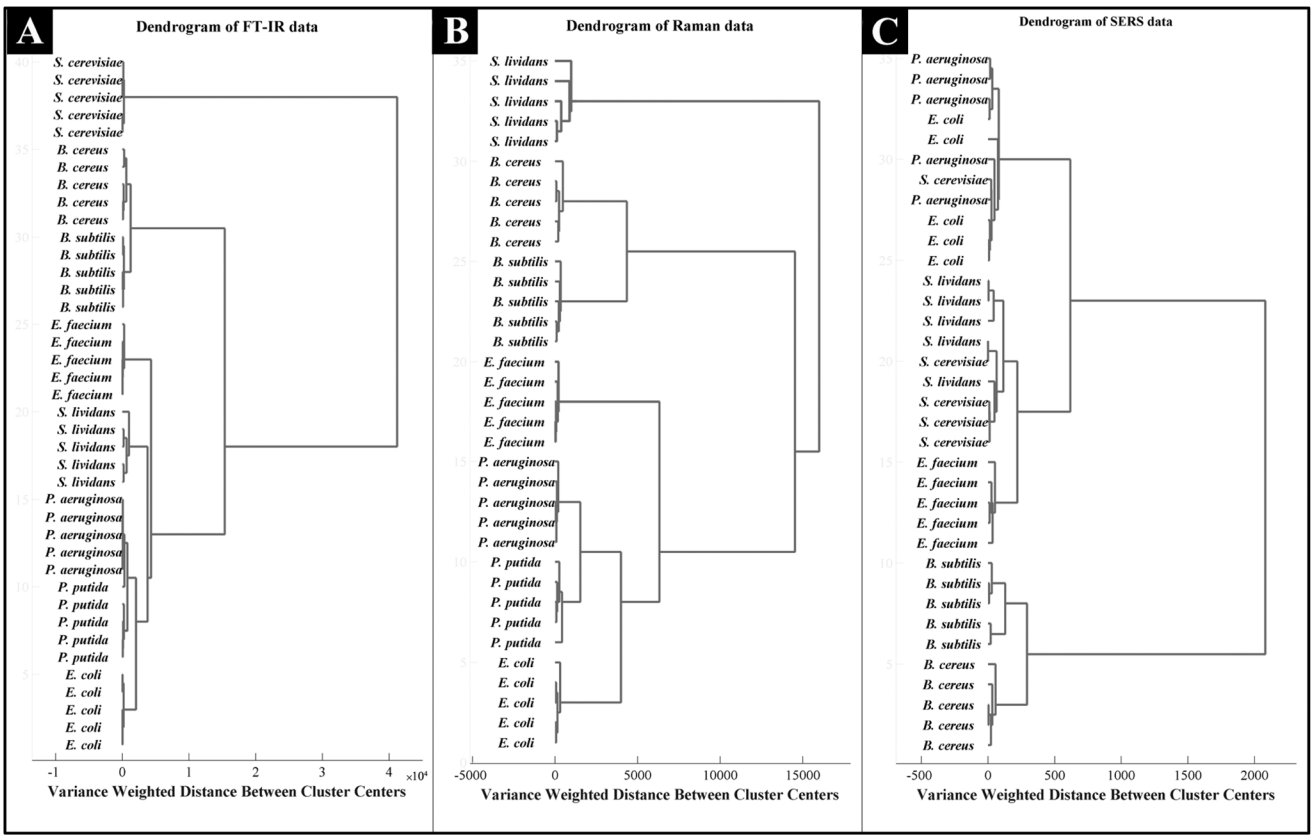

Fig. 5 Dendograms generated by HCA using means of the technical replicates from each of the bio-replicates (n = 5) of different classes (species) of samples for: FT-IR (A), Raman (B), and SERS (C) spectral data.

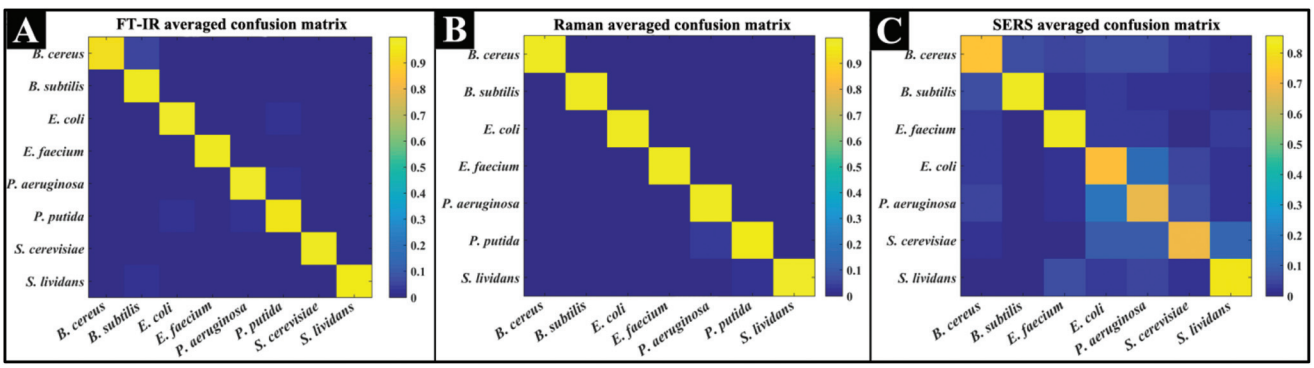

Fig. 6 The averaged confusion matrices of the classification models generated using PLS-DA and validated by bootstrapping method (1000 iterations), of the FT-IR (A), Raman (B), and SERS (C) spectral data.

pared to that of the FT-IR and Raman models, with an average prediction accuracy of 74.9% (Table S3†). This may be expected given the observations of the cluster compactness seen in Fig. 4 for the three spectroscopies.

Discussion

Accurate detection and identification of microorganisms is of great interest with a wide range of existing and potential applications, including: pharmaceutical manufacturing processes, food quality control, medicine, environmental monitoring and bioremediation, and synthetic biology. For example, the early detection of pathogens in clinical microbiology laboratories (or indeed in general practice) may accelerate the initiation of appropriate and targeted treatment,[79] which may prevent the development of future challenges such as antibiotic resistance.[80,81]

During the past two decades, vibrational spectroscopic techniques have demonstrated great potential for this task,[82] which has also been reflected by the development of various

commercial systems (*e.g.* River Diagnostics (http://www.riverd.com), and rapID (http://www.rap-id.com) Particle Systems GmbH). Although IR, Raman and SERS spectroscopic techniques have been successfully applied for microbial characterisation and identification, the question remains, which is the most appropriate technique?

Thus, the aim of this study was to compare, and demonstrate the applicability and accuracy of FT-IR, Raman and SERS, as physicochemical whole organism fingerprinting approaches, for differentiation of a range of microbial samples. While the collected spectra of bacteria and yeast cells investigated in this study shared similar spectral bands (Fig. 3), it was shown using multivariate analyses that the relative intensities of these bands were specific to each of the species and strains, which allowed for the differentiation of the samples (Fig. 5). Furthermore, the relative clustering pattern of *S. lividans* to *S. cerevisiae* on the FT-IR PC-DFA scores plot (Fig. 4B), and *S. lividans* to *Pseudomonas* spp. on the Raman PC-DFA scores plot (Fig. 4D), emphasises that these clustering patterns are not dependant on the different incubation temperatures and growth conditions used in this study, but due to other phenotypic/biochemical differences.

The PLS-DA classification models generated using FT-IR and Raman spectral data provided highly accurate prediction values of 96.2% and 97.8% respectively, allowing for the differentiation of yeast from bacterial cells, and further discrimination of bacterial cells down to sub-species level (Fig. 5A and B). However, the background fluorescence from *S. cerevisiae* in the resultant 'Raman' spectra led to the exclusion of these samples from the subsequent modelling process. Nonetheless, the spectra collected from both techniques clearly demonstrated their complementarity (Fig. S4†), while the overall clustering patterns were also in agreement. Although, the SERS classification model had lower prediction accuracy (average of 74.9%), it displayed unique clustering patterns which allowed for the ready differentiation of Gram-positive and Gram-negative bacterial samples. This is perhaps not surprising as the AgNPs are in the vicinity of the cell membrane, which allows for the enhancement of the Raman signal from the outer surface, providing structural information and subsequently differentiation.[19,55]

One of several interesting observations from this study was that spectral data from all three vibrational spectroscopic techniques resulted in a clear separation of *Bacillus* spp., from all other bacterial samples that were analysed. This could be the result of any number of factors of course, though we consider this separation is probably to be due to differences in biochemical composition of the bacterial cell membrane (mainly protein, RNA and lipids),[83,84] or the cell wall peptidoglycan building blocks (*N*-acetyl-D-glucosamine and *N*-acetylmuramic acid), which is also evident (730 cm^{-1}) from DF1 loadings plot (Fig. S2C†) of the SERS spectral data.[55,85]

It is also worth noting that whilst numerous studies have demonstrated the potential applications of Raman and SERS for analysis of biological samples;[86,87] the application of these exceptionally useful techniques require careful consideration and choice of instrument, instrumental parameters, and of course experimental design[88] (*e.g.* choice of laser excitation wavelength), prior to their application to a specific type of biological sample. Here for example, using our comparative approach, it was found that whilst background fluorescence was observed from Raman spectra for *S. cerevisiae*, this fluorescence quenched when applying SERS to the same species, and conversely SERS appeared to introduce strong fluorescence when analysing *P. putida*. Furthermore, whilst it is well known that mid-infrared is a strong absorber of water, after drying samples for a short period prior to analysis, FT-IR spectra were shown to provide for a highly reproducible and accurate classification model for the whole range of samples used in this study. Thus, despite the limited number of microorganisms examined, the findings of this study suggest FT-IR as ideal method for differentiation of microorganisms in pure, or potentially mixed cultures.

In conclusion, this combined and comparative study of a range of clinically and industrially relevant microorganisms, clearly demonstrates the potential application of Raman, SERS, and FT-IR spectroscopies for microbial classification and differentiation. Although this is perhaps not surprising, given the rapidly expanding literature regarding individual applications of each of the three techniques explored here.[89–91] The opposite observation is that our findings bring into focus and highlight the fact that when compared directly, there is not '*one method fits all*'. Indeed, careful thought is required prior to selection of one or more of these techniques, especially regarding sample type, format, preparation, and the biological questions being asked. These spectroscopies, individually or when combined, will continue to reveal much detailed and useful knowledge, and enable novel insights into biological systems and bioprocesses, though only if applied correctly. Finally, these rapid methods, with their potential to be combined within single benchtop, bedside, or handheld portable units,[29] and continued advances in miniaturisation, computation, and materials, only increases their potential into an ever expanding horizon of biological, clinical, and industrial microbiological applications.

Acknowledgements

HM and RG thank the European Commission's Seventh Framework Program for funding (STREPSYNTH; Project No. 613877). MM acknowledges Commonwealth of Australia for an Endeavour Research Award to visit University of Manchester (award 4660_2015). XY thanks the Cancer Research UK for funding (including an Experimental Cancer Medicine Centre award). RG is also very grateful to BBSRC for financial support and, in particular, for Raman microscopy (BB/L014823/1). VB acknowledges Australian Research Council for an ARC Future Fellowship (FT140101285) and the Ian Potter Foundation for establishing an Ian Potter NanoBioSensing Facility at RMIT University, which is directed towards developing new international linkages with Australia in the area of nano-

 This journal is © The Royal Society of Chemistry 2016

diagnostics. RR acknowledges RMIT University for a Vice Chancellor's Postdoctoral Research Fellowship.

References

1 J. D. G. Jones and J. L. Dangl, *Nature*, 2006, **444**, 323–329.
2 L. A. David, C. F. Maurice, R. N. Carmody, D. B. Gootenberg, J. E. Button, B. E. Wolfe, A. V. Ling, A. S. Devlin, Y. Varma, M. A. Fischbach, S. B. Biddinger, R. J. Dutton and P. J. Turnbaugh, *Nature*, 2014, **505**, 559–563.
3 E. Sherr and B. Sherr, *Limnol. Oceanogr.*, 1988, **33**, 1225–1227.
4 S. Chu and A. Majumdar, *Nature*, 2012, **488**, 294–303.
5 Z. Du, H. Li and T. Gu, *Biotechnol. Adv.*, 2007, **25**, 464–482.
6 A. L. Juhasz and R. Naidu, *Int. Biodeterior. Biodegrad.*, 2000, **45**, 57–88.
7 T. C. Hazen, E. A. Dubinsky, T. Z. DeSantis, G. L. Andersen, Y. M. Piceno, N. Singh, J. K. Jansson, A. Probst, S. E. Borglin, J. L. Fortney, W. T. Stringfellow, M. Bill, M. E. Conrad, L. M. Tom, K. L. Chavarria, T. R. Alusi, R. Lamendella, D. C. Joyner, C. Spier, J. Baelum, M. Auer, M. L. Zemla, R. Chakraborty, E. L. Sonnenthal, P. D'Haeseleer, H. Y. N. Holman, S. Osman, Z. M. Lu, J. D. Van Nostrand, Y. Deng, J. Z. Zhou and O. U. Mason, *Science*, 2010, **330**, 204–208.
8 D. I. Ellis and R. Goodacre, *Curr. Opin. Biotechnol*, 2012, **23**, 22–28.
9 H. S. Toogood, S. Tait, A. Jervis, A. Ní Cheallaigh, L. Humphreys, E. Takano, J. M. Gardiner and N. S. Scrutton, in *Methods in Enzymology*, Academic Press, 2016, DOI: 0.1016/bs.mie.2016.02.020.
10 S. Brul and P. Coote, *Int. J. Food Microbiol.*, 1999, **50**, 1–17.
11 L. Gram, L. Ravn, M. Rasch, J. B. Bruhn, A. B. Christensen and M. Givskov, *Int. J. Food Microbiol.*, 2002, **78**, 79–97.
12 F. Baquero, J.-L. Martinez and R. Canton, *Curr. Opin. Biotechnol.*, 2008, **19**, 260–265.
13 D. J. Barker and D. C. Stuckey, *Water Res.*, 1999, **33**, 3063–3082.
14 C. Kirschner, K. Maquelin, P. Pina, N. A. Ngo Thi, L. P. Choo-Smith, G. D. Sockalingum, C. Sandt, D. Ami, F. Orsini, S. M. Doglia, P. Allouch, M. Mainfait, G. J. Puppels and D. Naumann, *J. Clin. Microbiol.*, 2001, **39**, 1763–1770.
15 I. Vliegen, J. A. Jacobs, E. Beuken, C. A. Bruggeman and C. Vink, *J. Microbiol. Methods*, 2006, **66**, 156–164.
16 R. I. Amann, W. Ludwig and K. H. Schleifer, *Microbiol. Rev.*, 1995, **59**, 143–169.
17 D. Dubois, D. Leyssene, J. P. Chacornac, M. Kostrzewa, P. O. Schmit, R. Talon, R. Bonnet and J. Delmas, *J. Clin. Microbiol.*, 2010, **48**, 941–945.
18 H. Muhamadali, D. Weaver, A. Subaihi, N. AlMasoud, D. K. Trivedi, D. I. Ellis, D. Linton and R. Goodacre, *Analyst*, 2016, **141**, 111–122.
19 R. M. Jarvis and R. Goodacre, *Chem. Soc. Rev.*, 2008, **37**, 931–936.
20 S. Efrima and L. Zeiri, *J. Raman Spectrosc.*, 2009, **40**, 277–288.
21 B. C. Smith, *Fundamentals of Fourier transform infrared spectroscopy*, CRC Press, Boca Raton, FL, 2011.
22 L. E. Rodriguez-Saona, F. M. Khambaty, F. S. Fry, J. Dubois and E. M. Calvey, *J. Food Prot.*, 2004, **67**, 2555–2559.
23 D. I. Ellis, D. Broadhurst, D. B. Kell, J. J. Rowland and R. Goodacre, *Appl. Environ. Microbiol.*, 2002, 68.
24 H. Muhamadali, Y. Xu, D. I. Ellis, J. W. Allwood, N. J. W. Rattray, E. Correa, H. Alrabiah, J. R. Lloyd and R. Goodacre, *Appl. Environ. Microbiol.*, 2015, **81**, 3288–3298.
25 H. Muhamadali, Y. Xu, D. I. Ellis, D. K. Trivedi, N. J. W. Rattray, K. Bernaerts and R. Goodacre, *Microb. Cell Fact.*, 2015, 14.
26 H. Muhamadali, Y. Xu, R. Morra, D. K. Trivedi, N. J. W. Rattray, N. Dixon and R. Goodacre, *Mol. BioSyst.*, 2016, **12**, 350–361.
27 E. S. Wharfe, R. M. Jarvis, C. L. Winder, A. S. Whiteley and R. Goodacre, *Environ. Microbiol.*, 2010, **12**, 3253–3263.
28 H. Wang, K. Hollywood, R. M. Jarvis, J. R. Lloyd and R. Goodacre, *Appl. Environ. Microbiol.*, 2010, **76**, 6266–6276.
29 D. I. Ellis, H. Muhamadali, S. A. Haughey, C. T. Elliott and R. Goodacre, *Anal. Methods*, 2015, **7**, 9401–9414.
30 D. I. Ellis, D. P. Cowcher, L. Ashton, S. O'Hagan and R. Goodacre, *Analyst*, 2013, **138**, 3871–3884.
31 D. Kusic, B. Kampe, P. Roesch and J. Popp, *Water Res.*, 2014, **48**, 179–189.
32 S. Meisel, S. Stoeckel, M. Elschner, F. Melzer, P. Roesch and J. Popp, *Appl. Environ. Microbiol.*, 2012, **78**, 5575–5583.
33 S. Meisel, S. Stoeckel, P. Roesch and J. Popp, *Food Microbiol.*, 2014, **38**, 36–43.
34 K. Sowoidnich, H. Schmidt, H.-D. Kronfeldt and F. Schwaegele, *Vib. Spectrosc.*, 2012, **62**, 70–76.
35 L. P. Choo-Smith, H. G. M. Edwards, H. P. Endtz, J. M. Kros, F. Heule, H. Barr, J. S. Robinson, H. A. Bruining and G. J. Puppels, *Biopolymers*, 2002, **67**, 1–9.
36 S. Kloss, B. Kampe, S. Sachse, P. Roesch, E. Straube, W. Pfister, M. Kiehntopf and J. Popp, *Anal. Chem.*, 2013, **85**, 9610–9616.
37 W. E. Huang, A. D. Ward and A. S. Whiteley, *Environ. Microbiol. Rep.*, 2009, **1**, 44–49.
38 L. P. Choo-Smith, K. Maquelin, T. van Vreeswijk, H. A. Bruining, G. J. Puppels, N. A. Ngo Thi, C. Kirschner, D. Naumann, D. Ami, A. M. Villa, F. Orsini, S. M. Doglia, H. Lamfarraj, G. D. Sockalingum, M. Manfait, P. Allouch and H. P. Endtz, *Appl. Environ. Microbiol.*, 2001, **67**, 1461–1469.
39 K. Maquelin, L. P. Choo-Smith, T. van Vreeswijk, H. P. Endtz, B. Smith, R. Bennett, H. A. Bruining and G. J. Puppels, *Anal. Chem.*, 2000, **72**, 12–19.
40 J. W. Chan, A. P. Esposito, C. E. Talley, C. W. Hollars, S. M. Lane and T. Huser, *Anal. Chem.*, 2004, **76**, 599–603.
41 H. Muhamadali, M. Chisanga, A. Subaihi and R. Goodacre, *Anal. Chem.*, 2015, **87**, 4578–4586.

42 W. E. Huang, R. I. Griffiths, I. P. Thompson, M. J. Bailey and A. S. Whiteley, *Anal. Chem.*, 2004, **76**, 4452–4458.
43 C. Xie, J. Mace, M. A. Dinno, Y. Q. Li, W. Tang, R. J. Newton and P. J. Gemperline, *Anal. Chem.*, 2005, **77**, 4390–4397.
44 W. E. Huang, M. Li, R. M. Jarvis, R. Goodacre and S. A. Banwart, in *Advances in Applied Microbiology*, Academic Press, 2010, vol. 70, pp. 153–186.
45 M. Fleischmann, P. J. Hendra and A. J. McQuillan, *Chem. Phys. Lett.*, 1974, **26**, 163–166.
46 S. McAughtrie, K. Faulds and D. Graham, *J. Photochem. Photobiol., C*, 2014, **21**, 40–53.
47 A. F. Chrimes, K. Khoshmanesh, P. R. Stoddart, A. A. Kayani, A. Mitchell, H. Daima, V. Bansal and K. Kalantar-zadeh, *Anal. Chem.*, 2012, **84**, 4029–4035.
48 J. A. Dougan, D. MacRae, D. Graham and K. Faulds, *Chem. Commun.*, 2011, **47**, 4649–4651.
49 D. Graham, R. Stevenson, D. G. Thompson, L. Barrett, C. Dalton and K. Faulds, *Faraday Discuss.*, 2011, **149**, 291–299.
50 D. van Lierop, I. A. Larmour, K. Faulds and D. Graham, *Anal. Chem.*, 2013, **85**, 1408–1414.
51 I. A. Larmour, K. Faulds and D. Graham, *Chem. Sci.*, 2010, **1**, 151–160.
52 R. Stevenson, S. McAughtrie, L. Senior, R. J. Stokes, H. McGachy, L. Tetley, P. Nativo, J. M. Brewer, J. Alexander, K. Faulds and D. Graham, *Analyst*, 2013, **138**, 6331–6336.
53 H. Zhou, D. Yang, N. P. Ivleva, N. E. Mircescu, R. Niessner and C. Haisch, *Anal. Chem.*, 2014, **86**, 1525–1533.
54 K. Gracie, E. Correa, S. Mabbott, J. A. Dougan, D. Graham, R. Goodacre and K. Faulds, *Chem. Sci.*, 2014, **5**, 1030–1040.
55 R. M. Jarvis and R. Goodacre, *Anal. Chem.*, 2004, **76**, 40–47.
56 L. Zeiri and S. Efrima, *J. Raman Spectrosc.*, 2005, **36**, 667–675.
57 L. Cui, Y.-J. Zhang, W. E. Huang, B.-F. Zhang, F. L. Martin, J.-Y. Li, K.-S. Zhang and Y.-G. Zhu, *Anal. Chem.*, 2016, **88**, 3164–3170.
58 S. Schlücker, *Angew. Chem., Int. Ed.*, 2014, **53**, 4756–4795.
59 A. P. Craig, A. S. Franca and J. Irudayaraj, *Annu. Rev. Food Sci. Technol.*, 2013, **4**, 369–380.
60 M. Vendrell, K. K. Maiti, K. Dhaliwal and Y.-T. Chang, *Trends Biotechnol.*, 2013, **31**, 249–257.
61 C. L. Winder, S. V. Gordon, J. Dale, R. G. Hewinson and R. Goodacre, *Microbiology*, 2006, 152.
62 R. J. Barnes, M. S. Dhanoa and S. J. Lister, *Appl. Spectrosc.*, 1989, **43**, 772–777.
63 P. R. Selvakannan, R. Ramanathan, B. J. Plowman, Y. M. Sabri, H. K. Daima, A. P. O'Mullane, V. Bansal and S. K. Bhargava, *Phys. Chem. Chem. Phys.*, 2013, **15**, 12920–12929.
64 H. K. Daima, P. R. Selvakannan, R. Shukla, S. K. Bhargava and V. Bansal, *PLoS One*, 2013, **8**, e79676.
65 T. Cosgrove, *Colloid Science: Principles, Methods and Applications*, 2005.
66 R. C. Maher, in *Raman Spectroscopy for Nanomaterials Characterization*, ed. C. S. S. R. Kumar, Springer, Berlin Heidelberg, 2012, pp. 215–260, DOI: 10.1007/978-3-642-20620-7_10.
67 M. Hubert, P. Rousseeuw and T. Verdonck, *Comput. Stat. Data Anal.*, 2009, **53**, 2264–2274.
68 H. J. H. Macfie, C. S. Gutteridge and J. R. Norris, *J. Gen. Microbiol.*, 1978, **104**, 67–74.
69 P. S. Gromski, H. Muhamadali, D. I. Ellis, Y. Xu, E. Correa, M. L. Turner and R. Goodacre, *Anal. Chim. Acta*, 2015, **879**, 10–23.
70 B. Efron and G. Gong, *Am. Stat.*, 1983, **37**, 36–48.
71 N. AlMasoud, Y. Xu, N. Nicolaou and R. Goodacre, *Anal. Chim. Acta*, 2014, **840**, 49–57.
72 S. A. Patel, F. Currie, N. Thakker and R. Goodacre, *Analyst*, 2008, **133**, 1707–1713.
73 A. D. Shaw, N. Kaderbhai, A. Jones, A. M. Woodward, R. Goodacre, J. J. Rowland and D. B. Kell, *Appl. Spectrosc.*, 1999, **53**, 1419–1428.
74 G. McNay, D. Eustace, W. E. Smith, K. Faulds and D. Graham, *Appl. Spectrosc.*, 2011, **65**, 825–837.
75 S. C. Kachlany, S. B. Levery, J. S. Kim, B. L. Reuhs, L. W. Lion and W. C. Ghiorse, *Environ. Microbiol.*, 2001, **3**, 774–784.
76 J. Guicheteau, L. Argue, D. Emge, A. Hyre, M. Jacobson and S. Christesen, *Appl. Spectrosc.*, 2008, **62**, 267–272.
77 Y. Chao and T. Zhang, *Anal. Bioanal. Chem.*, 2012, **404**, 1465–1475.
78 M. Kahraman, A. I. Zamaleeva, R. F. Fakhrullin and M. Culha, *Anal. Bioanal. Chem.*, 2009, **395**, 2559–2567.
79 D. I. Ellis, W. B. Dunn, J. L. Griffin, J. W. Allwood and R. Goodacre, *Pharmacogenomics*, 2007, **8**, 1243–1266.
80 S. B. Levy, *The Antibiotic Paradox: How the Misuse of Antibiotics Destroys Their Curative Powers*, Perseus Pub., 2002.
81 B. M. Marshall and S. B. Levy, *Clin. Microbiol. Rev.*, 2011, **24**, 718–733.
82 M. Harz, P. Rosch and J. Popp, *Cytometry, Part A*, 2009, **75**, 104–113.
83 D. G. Bishop, L. Rutberg and B. Samuelss, *Eur. J. Biochem.*, 1967, **2**, 448–453.
84 C. Sohlenkamp and O. Geiger, *FEMS Microbiol. Rev.*, 2016, **40**, 133–159.
85 R. M. Jarvis, A. Brooker and R. Goodacre, *Faraday Discuss.*, 2006, **132**, 281–292; discussion 309-219.
86 M. J. Baker, S. R. Hussain, L. Lovergne, V. Untereiner, C. Hughes, R. A. Lukaszewski, G. Thiefin and G. D. Sockalingum, *Chem. Soc. Rev.*, 2016, **45**, 1803–1818.
87 S. Mabbott, D. Thompson, N. Sirimuthu, G. McNay, K. Faulds and D. Graham, *Faraday Discuss.*, 2016, **187**, 461–472.
88 H. Fisk, C. Westley, N. J. Turner and R. Goodacre, *J. Raman Spectrosc.*, 2016, **47**, 59–66.
89 R. Hou, S. Pang and L. He, *Anal. Methods*, 2015, **7**, 6325–6330.
90 C. Hughes and M. J. Baker, *Analyst*, 2016, **141**, 467–475.
91 M. J. Baker and K. Faulds, *Chem. Soc. Rev.*, 2016, **45**, 1792–1793.

This journal is © The Royal Society of Chemistry 2016